# Reactive scattering of $NH_3^+$ (v, J) ions at film covered indium tin oxide (ITO) surfaces

Thomas Kolling, Shutao Sun, Karl-Michael Weitzel *

*Fachbereich Chemie, Physikalische Chemie; Philipps-Universität Marburg, Marburg, Germany*

### ARTICLE INFO

### ABSTRACT

We describe the setup of an experiment for the investigation of ion-surface reactions with time of flight analysis of products. It consists of an ion source where state-selected ammonia ions $NH_3^+$ (v, J) are formed by resonance enhanced multi-photon ionization ((2 + 1) REMPI). The ions are guided to a scattering chamber where the interaction with an indium tin oxide (ITO) surface covered by a layer of H-atoms containing neutral molecules can be investigated as a function of the kinetic energy. Product yields are analyzed in a time of flight mass spectrometer (TOF). The characteristics of the experiment are illustrated by the help of SIMION trajectory calculations. We show that at impact energies around 15 eV pick up of H atoms from the layer occurs. At higher impact energies, around 30 eV, dissociative scattering of ammonia ions dominates. Collision energy resolved mass spectra (CERMS) are presented. The TOF analysis indicates an ammonia molecular layer as the origin for H abstraction in accordance with the experimental conditions.

© 2008 Elsevier B.V. All rights reserved.

## 1. Introduction

The interaction between molecular ions and surfaces is of considerable interest in many fields of science and technology [1]. In particular the modification of surfaces and their analysis via interactions with ions and the production or modification of thin films at surfaces attracted considerable attention [2]. Here, the different processes involved may be classified according to the impact energy or the velocity of the ions being scattered, respectively. In general four different energy ranges are distinguished.

The so-called thermal energy range (up to approximately 1 eV) is dominated by elastic scattering, physisorption and dissociative chemisorption [3]. Here, the internal degrees of freedom (vibration and rotation) can have significant impact on the cross-sections. Important information can be achieved by means of experiments with ions in well-defined quantum states [4,5]. In the hyperthermal energy range (1 eV up to several tens of eV) the impact energy exceeds typical chemical binding energies. Therefore the translational energy is large enough to induce pronounced chemical changes at and in the surface. However, in general it is still not large enough to modify the surface itself. Processes of modifica-

tion occur at impact energies of several hundred eV. From the chemical point of view it is the hyperthermal range, which is most appealing. Numerous reports are dealing with the fundamental aspects of chemical interaction between molecular ions and atomic monolayers or self assembled monolayers [6–8]. Between 1 and 10 keV ion scattering is accompanied by sputtering of target material. Analytical applications include the ion scattering spectrometry (ISS), the secondary ion mass spectrometry (SIMS) [9] and time of flight secondary ion mass spectrometry (TOF-SIMS) [10] as technique for surface analysis, although at the cost of material destruction.

Within this energy range implantation of ions into the substrate plays an important role providing access to modification of material properties (plasma etching, etc.). At even higher energy (MeV range) Rutherford backscattering occurs.

Apart from the chemical motivation work in the hyperthermal range is also stimulated by fusion research. This is due to the specific interaction of plasma ions with reactor walls. Typical experiments have focused on the interaction of $D_3^+$ at target material leading to the formation of $D^+$, $D_2^+$ and $D_3^+$ [11]. Here, one central process involves surface induced dissociation (SID). SID is also an important process in the interaction of cluster ions with surfaces [12]. In general the elementary processes of hyperthermal ions can be subdivided, as depicted in Fig. 1, into elastic and inelastic scattering (1a), neutralization (1b), adsorption (1c), reactive scattering (1d and

---

* Corresponding author.
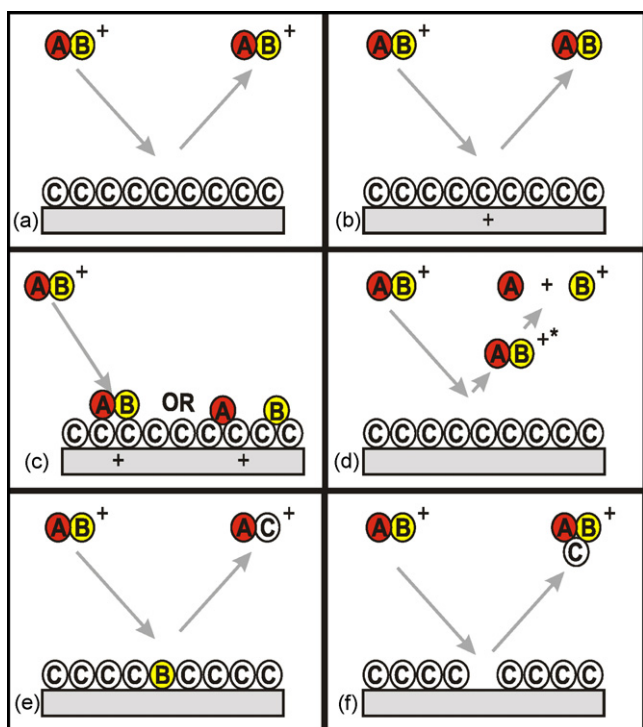  *E-mail address:* weitzel@chemie.uni-marburg.de (K.-M. Weitzel).

**Fig. 1.** Different molecular ion surface interaction in the hyperthermal energy region.

1e), and pick up scattering (1f). Processes 1a, 1d and 1f are explicitly discussed in this work.

From the chemical point of view the pure elastic scattering does not provide significant new information. In quasi-elastic processes, on the other hand, internal degrees of freedom can be excited, and can ultimately lead to SID, etc. Experiments regarding the redistribution of impact energy to internal degrees of freedom have, e.g., been reported by Märk and Herman [13].

Relatively little is known on the influence of quantum states of projectile ions on the yield of reactive scattering products [14,15]. In this contribution we describe experiments particularly aimed at the reactive scattering of quantum state selected ammonia ions, $NH_3{}^+(v, J)$, from an indium tin oxide (ITO; $In_2O_3$:$SnO_2$) surface covered with a monolayer of neutral residual gas (97% of which is ammonia).

ITO is an electrically conductive and optically transparent material with high transmission in the visible and near IR range. Areas of application are the display technology, transparent electrodes, ITO coated slides, microstructure technology, high frequency screen, optically permeable heating glass, electroluminescent displays, invisible antennas from ITO glass, optical heating tables, snow and ice removal devices, heatable object-slow-acting, etc. In the context of the current work the use of an ITO sample as target material is interesting for at least two reasons. For semiconductors and oxides the process of the neutralization [16] is smaller, than for classical metallic target surfaces [17–22]. In our experiment this would suggest higher ion counting rates. Typical commercial samples are characterized by a small micro-roughness within the nm range and a very good homogeneity of the surface resistance. Since ITO is a conductive material direct electrical contacting and thus control of electrostatic fields at the target are possible.

The sample employed in this work (typ CEC020S) has been purchased from pgo Inc. (Präzisions Glas & Optik) as a 100-nm thin ITO layer with a surface resistance of $R < 20\,\Omega/cm^2$ deposited on top of
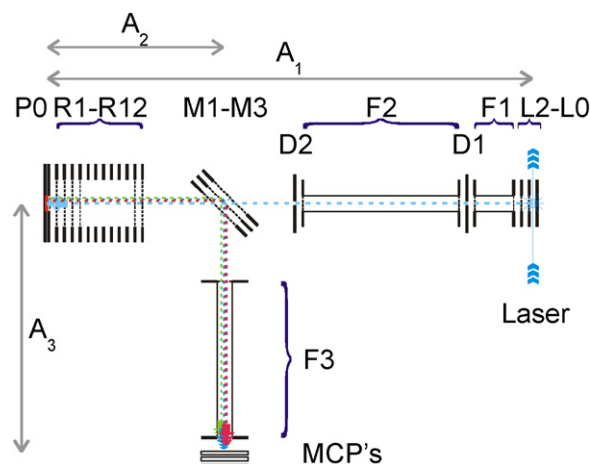


**Fig. 2.** Schematic view of the setup with labels for the electrostatic lenses (L0–L2), the electrostatic mirror (M1–M3) and reflector with sample holder (R1–R12, P0). $A_1$, $A_2$ and $A_3$ mark the path taken by ions from the ion source to the sample, from the sample to the mirror, and from the mirror to the detector, where F3 and the MCP's builds the TOF-spectrometer, respectively.

a thin passivation layer of $SiO_2$ which in turn was deposited on a $2\,cm \times 2\,cm \times 0.11\,cm$ floating glass substrate.

## 2. Experimental setup

This section describes the setup of the apparatus dedicated to the reactive scattering of state-selected molecular ions at surfaces. The schematic view of the spectrometer is shown in Fig. 2.

The ions were formed in a laser ionization process in the ion chamber (L0–L2, flight tube F1) and transferred via the path A1 to the reaction chamber. After interaction with the sample at P0 the resulting positive ions are accelerated in the electrostatic field of the reflector (R1–R12), reflected at the electrostatic mirror (M1–M3), transferred to the TOF-spectrometer via the paths A2–A3 and detected at the MCP's.

In detail the Ammonia ions are formed in the centre of the ion source (between lenses L0 and L1) and subsequently accelerated towards the transfer chamber by means of static electric fields (typical draw out fields: 137 V/cm). The ions pass to field free drift tubes (F1 and F2) separated by pressure stage before entering into the scattering chamber. At the centre of the scattering chamber a freely rotatable electrostatic mirror is positioned, consisting of electrical lenses M1, M2, and M3. By applying the appropriate voltages this mirror is set to transmission or reflection, respectively. In the current experiment the mirror is operated in a pulsed modus. Let us consider a bunch of ions travelling towards the mirror. In order for the ion bunch to be able to penetrate the mirror, the latter needs to be set to the drift potential, in this case ground potential. After
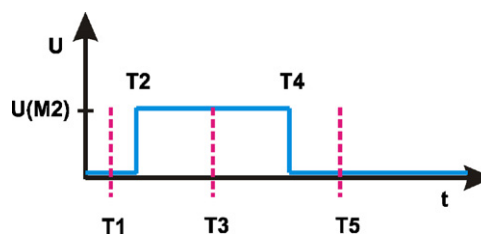


**Fig. 3.** Switching scheme of the electrostatic mirror (T1: ions passes el. stat. Mirror; T2: mirror switched on; T3: reflection of the ions at the mirror; T4: mirror switched off; T5: ions are detected at MCP's;). Mirror ready for transmission of next ion bunch.

being scattered at the sample surface the ion bunch (or any products) will move towards the mirror from the opposite side. At this point the mirror is being switched to a high potential, thus causing reflection of the ions into the time of flight mass spectrometer, also shown in Fig. 2.

The modus of pulsed operation of the mirror is depicted in Fig. 3.

For transmission of the ion bunch towards the reflector ground potential is applied to the electric lenses M1 to M3. The reflector consists of a system of 12 electrostatic lenses (R1 to R12) as well as the sample holder (P0). All lenses have circular openings with a diameter of 6 cm. The first four and the last two lenses are covered with galvanically formed copper meshes (InterNet Inc., type BM2000-03C, 95% transmission). Lenses R1 to R4 and R11 and R12 can be voltage adjusted independently. Lenses R4 to R11 are connected by a resistor chain consisting of 1 MΩ resistors each. By applying appropriate voltage to the lenses the kinetic energy of the ions can be adjusted between 0 V and about 2 keV with a resolution of about 100 meV. Subject to these conditions the ions can interact with the sample mounted in P0 between two stainless steel plates. The front plate has a central opening of 1 cm which exposes the sample to the ion beam. In order to minimize field inhomogeneities the sample is again covered by a mesh set to the same voltage as the sample itself. The potential of the sample can be adjusted independently. The rear plate is equipped with a heating device allowing us to apply temperatures up to about 1100 K to the sample. Impact of the ions onto the surface occurs under normal incidence. Reflection of the ions and the scattering processes are observed in the direction normal to the surface. Scattered ammonia ions as well as any product ions will be accelerated back through the reflector towards the mirror (as long as the sample potential is positive with respect to potential R1). At this point SIMION [23] simulations suggest no discrimination of backscattered ions. By switching the potential M2 at the mirror to a value positive compared to the laboratory ion energy the ions are reflected into the TOF mass spectrometer (F3) and subsequently detected by micro-channel plates.

This TOF is constructed according to the Wiley/McLaren type [24], c.f. Fig. 2. The laboratory energy of the primary ions is defined in the ion source. Lenses L0–L2 define a double stage acceleration, which focus the ions onto the sample. This focus is subsequently imaged onto the TOF-MS detector. The total time of flight of any ion detected will then consist of two contributions

$$t_{ion} = t_{A_1} + t_{A_2} + t_{A_3} \tag{1}$$

where $t_{A1}$ is the TOF of $NH_3^+$ ions from the source to the sample, and $t_{A2} + t_{A3}$ is the TOF of the scattered ion from the sample to the detector. The latter, of course depends on the mass of the scattered particle.

The vacuum system consists of three chambers: (i) the ion chamber, (ii) the transfer chamber, and (iii) the scattering chamber, all being differentially pumped by turbo molecular pumps. Typical operating pressures are on the order of $10^{-5}$ mbar in the ion source, $10^{-6}$ mbar in the transfer chamber, and $10^{-7}$ mbar in the scattering chamber. Under these conditions we estimate that any surface will be covered with a monolayer of the residual gas (here more than 97% is ammonia, other possible residuals could be hydrocarbons, water, etc.) after approximately 40 s.

Ammonia ions are formed in selected quantum states by (2 + 1) resonance enhanced multiphoton ionization (REMPI) [25] employing an excimer pumped dye laser utilizing the dye Rhodamin 101, with subsequent frequency doubling. Typical pulse energies are 500 μJ in the wavelength range 295–335 nm. The laser light is focused by a $f = 300$ mm lens. Ionization takes place in the centre of the ion source. Fig. 4 shows part of the (2 + 1) REMPI spectrum adapted from Ref. [25]. All experiments described in this work have been performed on the $Q_3(3)$ pump line in
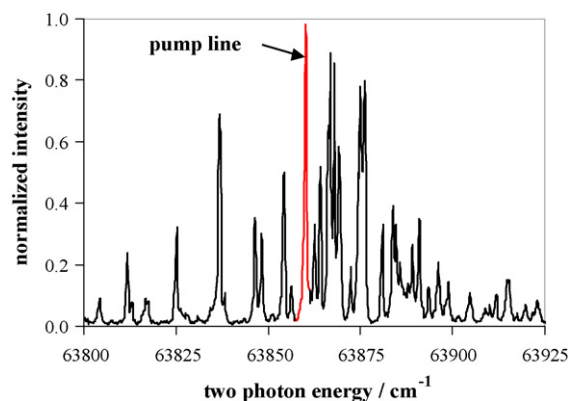


**Fig. 4.** (2 + 1) REMPI spectrum of the $\tilde{C}' \leftarrow \tilde{X} 2_{0+}^0$ band of the $NH_3$ [25].

the $\tilde{C}' \leftarrow \tilde{X} 2_{0+}^0$ band with $J = K = 3$, $\Delta J = \Delta K = 0$, at 63,860 cm$^{-1}$ (vacuum wavenumbers, corresponding to $\lambda = 313.095$ nm) [25,26].

## 3. Experimental results

First we describe results illustrating the time—and thus mass resolution of our setup. For this purpose ions are formed via the REMPI process discussed above at a laboratory potential of 1850 V and accelerated towards the electrostatic mirror. In this experiment the mirror is set at 45° angle relative to the incoming ion beam such that the ions are directly reflected into the TOF-MS (cf. Fig. 2). Reflection of the ions is here achieved by setting potential M2 to 2000 V. Fig. 5 shows a typical TOF-MS of primary ammonia ions recorded under these conditions. We note that the FWHM of the ion distribution is only 15 ns. Since ammonia is introduced via an effusive inlet, the sample is characterized by room temperature. According to theoretical estimates the thermal energy distribution leads to a broadening of the TOF distribution of approximately 8 ns full width half maximum (FWHM). Another contribution to the FWHM originates from the laser pulse duration which is on the order of 10 ns. Thus, we conclude that the TOF resolution is close to the theoretical limit. The actual TOF observed (9.34 μs) agrees very well with both analytical time of flight equations and SIMION trajectory calculations. The difference in the time of flight of $m/z = 17$ and $m/z = 18$ ions would be 270 ns, illustrating the mass resolution of the setup. The raw signal of the micro-channel plate detector has negative amplitude.
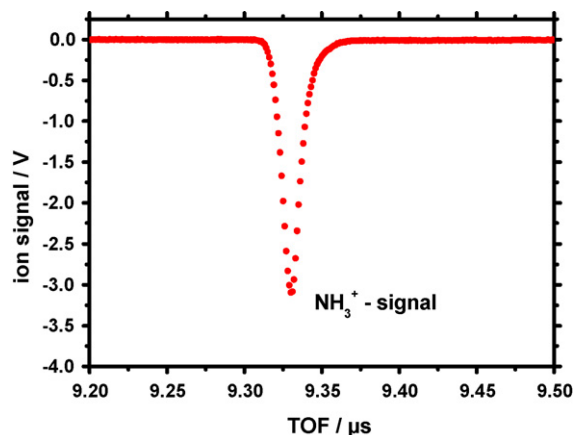


**Fig. 5.** Time of flight mass spectrum of $NH_3^+$ ions with direct reflection at the el. stat. mirror (M2 = 2000 V) into the TOF-MS; $t_{exp} = 9.331$ μs with FWHM $\Delta t_{exp} = 15$ ns.
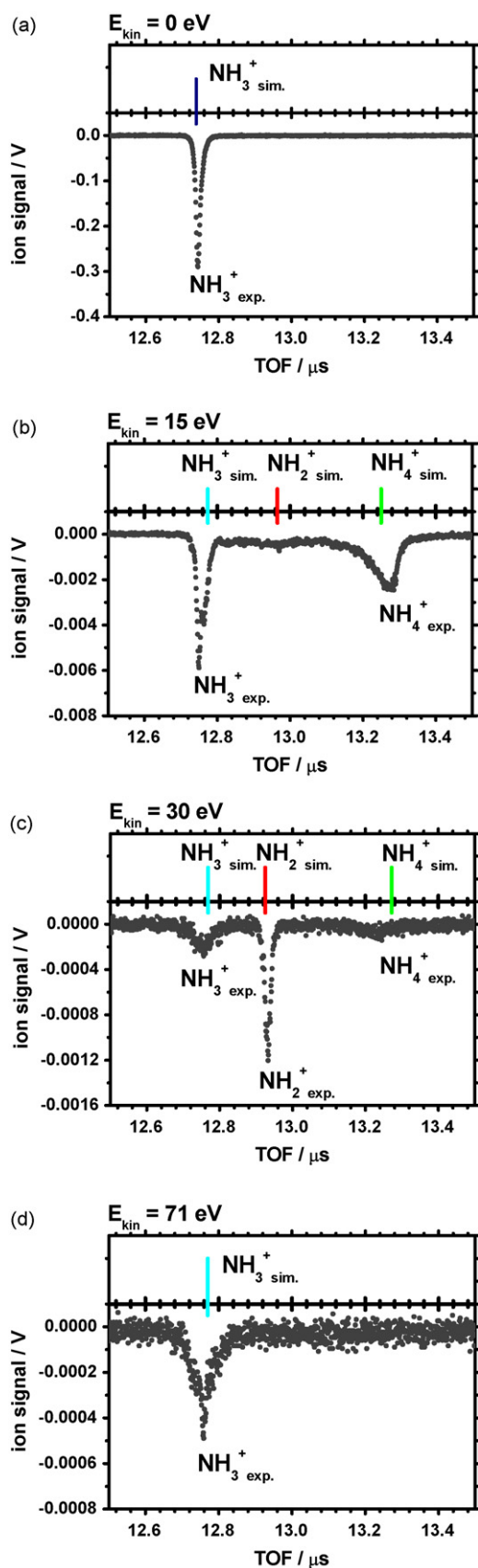
**Fig. 6.** (a) $NH_3^+$ ions with $E_{kin} \approx 0$ eV; (b) $NH_3^+$ ions with $E_{kin} = 15$ eV; (c) $NH_3^+$ ions with $E_{kin} = 30$ eV; (d) $NH_3^+$ ions with $E_{kin} = 71$ eV.

In the next section we describe results for scattering of ammonia ions from film covered ITO surface.

Throughout the rest of this work the lenses of the ion source are set to L1 = 1753 V, L1 = 1616 V and L2 = 0 V. For the actual position of the laser focus this leads to a birth potential of the ions of about 1655 V. The impact energy has been controlled via the voltage at P0 and referenced to the birth potential given above. The uncertainty in adjusting P0 is on the order of ±2 V. The lenses R1 to R12 are set to 0 V.

The electrostatic mirror is positioned at 135° with respect to the incoming beam of primary ions and operated in the pulsed modus described above. On the trajectory towards the reflector all mirror lenses are set to 0 V, on the backward trajectory lens M2 is pulsed to 2000 V, thus leading to reflection of all ions into the TOF-MS. Fig. 6a–d shows typical TOF mass spectra as a function of the impact energy. The only ions detected are assigned to $m/z$ = 16, 17, and 18. No indication of any traces of hydrocarbons has been observed.

Fig. 6a shows the TOF-MS for the impact energy of 0 eV, i.e., for ions reflected just in front of the surface without impinging on the surface. The latter conclusion is supported by (i) the signal amplitude (300 meV) and (ii) time of flight calculations. Only a single ion peak is observed under these conditions, clearly originating from intact ammonia ions. Upon increasing the impact energy to about 15 eV (Fig. 6b) we note a pronounced drop in the total ion signal (to about 6 meV), indicating that neutralization is an important process leading to a loss of about 98% of the incident ion intensity. Furthermore a second peak arises at this impact energy shifted by about 500 ns to larger TOF (13.3 μs). As we will support by model calculations (see below) this signal originates from $NH_4^+$ ions. These $NH_4^+$ ions are formed via H atom abstraction from a film covering the ITO surface. At even higher impact energy another peak emerges at 12.92 μs, which we attribute to $NH_2^+$ ions (Fig. 6b). The relative order of the TOF signals for $NH_3^+$, $NH_2^+$ and $NH_4^+$ originates from the different excess energies of the cations (see Section 4). The individual ion yields strongly depend on the impact energy. This is best illustrated in a plot of the relative ion yield as a function of the impact energy (see Fig. 7) usually termed CERMS diagram (collision energy resolved mass spectra).

Starting from 0 eV impact energy the relative ion yield of $NH_3^+$ decreases pronouncedly. In fact we may use this feature for calibrating the effective impact energy. With increasing impact energy first the relative yield of $NH_4^+$ ions increases, with a maximum relative yield of 50% at an impact energy of 15 eV. At even higher energy
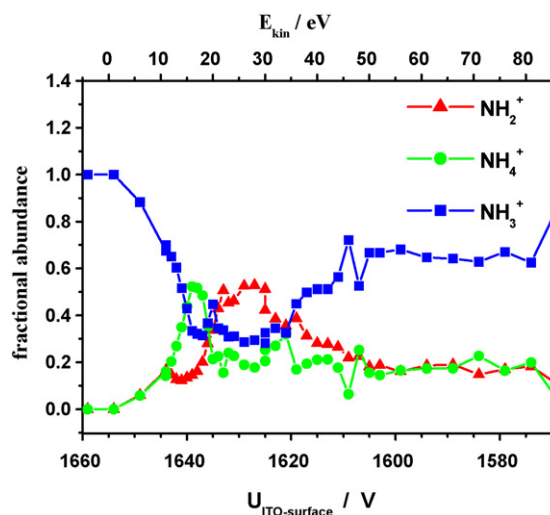


**Fig. 7.** CERMS diagram of the $NH_3^+$ scattered at ITO.

the yield of $NH_4^+$ ions decreases at the cost of $NH_2^+$ formation. The latter exhibits a maximum yield of again 50% around 20 eV impact energy. At the highest impact energies covered in this work the relative yield of reactive scattering products decreases. The remaining $NH_3^+$ signal (cf. Fig. 6d) can be rationalized by non-reactive reflection of $NH_3^+$ at the surface, as shown in model calculations below. However, we note, that the absolute scattering signal approaches the detection limit in this case. Thus the fractional abundances have to be viewed with caution above 50 eV impact energy.

## 4. Calculations and model

In the following we present a model rationalizing all ion signals observed based on energy partitioning in reactive scattering processes. No ions other than the three signals described above have been observed in the entire mass spectrum. The analysis is based on trajectory calculations employing the ion simulation program SIMION [23]. Four different scattering processes are being assumed to be operative; channel 1: neutralization (leading to loss of signal, since only ions are detected), channel 2: non-reactive scattering of $NH_3^+$, channel 3: formation of $NH_4^+$, and channel 4: formation of $NH_2^+$. An illustration of these channels is shown in Fig. 8. This sketch assumes that a monolayer of neutral ammonia is covering the ITO surface. Given the background pressure of $10^{-7}$ mbar $NH_3$ in the scattering chamber, this does indeed seem very plausible. We further assume that the lone electron pair of the adsorbed ammonia molecules points towards the surface [27]. Therefore the H atoms of the adsorbed ammonia points away from the surface, such that impinging ammonia ions will first interact with these H atoms leading to H atom pick up.

As mentioned before, among all these processes the cross-section is largest for neutralization (ch. 1) [21].

channel 1 :  $NH_3^+(v, J) + NH_{3,surf} \rightarrow 2NH_3(v^*, J^*)$  (3)
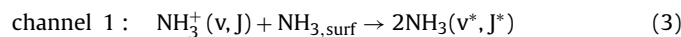
The second channel is due to inelastic scattering of $NH_3^+$ ions at the surface with partitioning of the kinetic energy between two ammonia molecules (Fig. 8, ch. 2).

channel 2 :  $NH_3^+(v, J) + NH_{3,surf} \rightarrow NH_3^+(v, J) + NH_3$  (4)
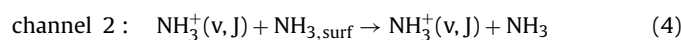
where

$$E_{kin\ out}(NH_3^+) = 0.5 \times E_{impact}$$  (5)

The third channel, i.e., H atom abstraction, is probably exothermic by about 920 meV in analogy with the corresponding gas phase reaction [28–30]. In our model we assume that this exothermicity correlates with the translational energy of the $NH_4^+$ ion being formed. The second product, neutral $NH_2$ is assumed to remain on
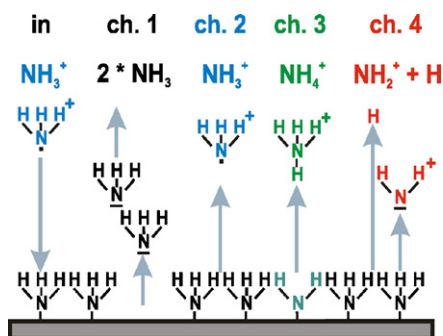


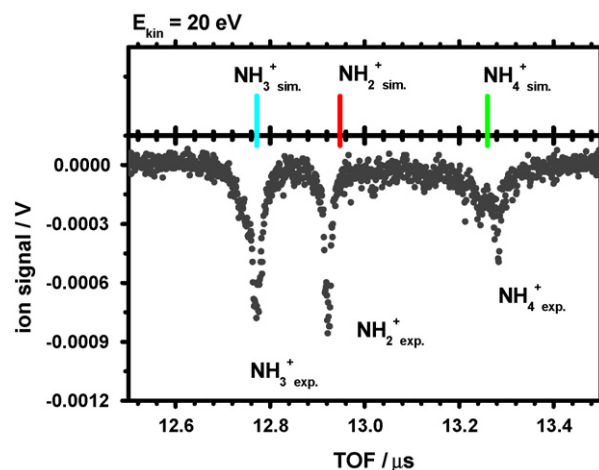**Fig. 8.** Model of the reaction channels of the interaction of $NH_3^+$ with a $NH_3$ monolayer on ITO.



**Fig. 9.** Comparison of the experimental time of flight spectra, obtained at $E_{impact} = 20$ eV, with SIMION trajectory calculations. For further details see the text.

the surface. Apparently the impact energy is dissipated into the surface film.

channel 3 :  $NH_3^+(v, J) + NH_{3,surf} \rightarrow NH_4^+(v^*, J^*) + NH_{2,surf}$  (6)
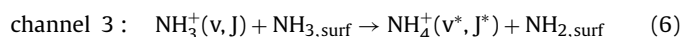
where

$$E_{kin}(NH_4^+) = E_{exoth}(NH_3^+(v, J) + NH_{3,surf}$$
$$\rightarrow NH_4^+(v^*, J^*) + NH_{2,surf})$$  (7)

The fourth channel corresponds to dissociative reactive scattering with formation of $NH_2^+$ ions. In a simple model the impact energy is partitioned between breaking one N–H bond and kinetic energy of the products being desorbed. According to the conservation of momentum the kinetic energy of $NH_2^+$ ions should amount to 1/17 of the excess energy $E_{excess} = E_{impact} - E_{bend-H}$. Thus, most of the excess energy is carried away by the hydrogen, leaving a relatively slow $NH_2^+$ ion. This ultimately leads to the TOF of $NH_2^+$ being larger than that of $NH_3^+$. At this point we assume that excitation of internal degrees of freedom does not play an important role.

channel 4 :  $NH_3^+(v, J) + NH_{3,surf} \rightarrow NH_2^+(v^*, J^*) + H + NH_{3,surf}$  (8)
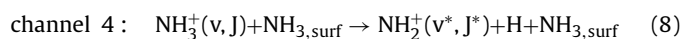
where

$$E_{kin}(NH_2^+) = 0.25 \times (E_{imp} - E_{diss}) \times \frac{1}{17}$$  (9)

Fig. 9 compares the experimental time of flight distribution obtained for an impact energy of 20 eV to the results of SIMION trajectory calculations, based on the model presented above. The expected TOF is also included in Fig. 6a–d. Evidently the calculated TOF in each case agrees very nicely with the experimental observation. This lends strong support to the interpretation of the data presented above. In particular the agreement between experiment and simulation clearly supports the assumption of an ammonia film being the origin for the scattering. Under background conditions of a scattering experiment surfaces are often contaminated by water or hydrocarbons. We have to stress, that we do not observe any ion signals other than the three signals in Fig. 9. Hydrocarbon ions are not compatible with these TOF spectra. Even the assumption of water being present in the layer would lead to ions of mass 18 and 19, basically being shifted from the observed ones by about 100 ns. Evidently the model of energy partitioning presented is capable of reproducing the experimental TOF's. Once additional information becomes available it could be easily included in the simulations discussed above.

## 5. Conclusion and outlook

We have investigated the reactive scattering of state-selected ammonia ions from an ITO surface covered with a layer of neutral molecules. Scattering products have been detected in a time of flight mass spectrometer. By comparison with theoretical TOF calculations three different ion signals have been assigned to (i) $NH_4^+$ (H-atom abstraction), (ii) $NH_3^+$ (non-reactive scattering), and (iii) $NH_2^+$ (dissociative scattering). We cannot strictly rule out contributions from other ions, however, the model presented in this work leads to the best agreement between experiment and simulation. The relative ion yields have been presented in a CERMS diagram. The analysis shows that H-atom abstraction plays an important role for collision energies in the range between thermal energies and about 15 eV. Neither we detect any hydrocarbon ions nor fragments of those. Under background conditions residual water or hydrocarbons could be present on the surface. However, under operating conditions of the experiment the surface will most likely be covered by an ammonia film. A TOF analysis has been presented based on the assumption that an ammonia film provides the H-atoms for the pick-up process. The agreement between experimental and theoretical TOF further supports our assumption. This represents in fact an application of the well-established TOF-SIMS technique [10]. Between 20 and 35 eV dissociative scattering leading to $NH_2^+$ ions dominates. The analysis was based on the assumption of ammonia molecules forming a monolayer on the ITO surface with the lone pair pointing towards the surface. Thus, the H atoms are exposed to the incoming ion beam and can eventually be abstracted. If one assumed the ammonia molecules were pointing with the H atoms towards the surface, H atom abstraction would hardly be possible. We therefore believe that the experiment described provides the possibility to analyze the binding conditions of very thin films covering a surface. For the future it would be interesting to further test this concept with surfaces, e.g., covered by a film of isotopically labeled ammonia, $ND_3$. These studies, however, are beyond the scope of this work.

The abstraction of H atoms from hydrocarbon covered steel surface has been the subject of several reports from Märk and coworkers. Wörgötter et al. [31] observed the pickup of H atoms by acetone in the range of collision energies between 10 and 20 eV, similar to the energy range of this work. Another report from the same group covered the abstraction of H atoms by benzene ions [32]. We note that the operating pressure in the work of Märk and coworkers was significantly lower than that in our work. This is most likely the reason why their work was limited by the background of hydrocarbons, in contrast to our work. While the current work and Ref. [31] indicate "resonance like" characteristics of H atom abstraction, the latter work did not show a pronounced energy dependence of this process. For the future it seems rewarding to further investigate these H atom pick up processes.

One of the advantages of REMPI preparation of ammonia ions pertains to the state-selectivity. This technique provides the possibility to form ions in different vibrational states or even different rotational states. It appears rewarding to investigate the role of internal degrees of freedom on the cross-sections for reactive scattering in future work. The current experiments are believed to be pivotal to plasma technical processes of reactive ion etching as well as surface film analysis.

## References

[1] Low Energy Ion-Surface Interactions: Wiley Series in Ion Chemistry and Physics, John Wiley and Sons Ltd., 1994.
[2] M.B.J. Wijesundara, L. Hanley, B.R. Ni, S.B. Sinnott, Proceedings of the National Academy of Sciences of the United States of America 97 (2000) 23.
[3] V. Grill, J. Shen, C. Evans, R.G. Cooks, Review of Scientific Instruments 72 (2001) 3149.
[4] P.R. Mccabe, L.B.F. Juurlink, A.L. Utz, Review of Scientific Instruments 71 (2000) 42.
[5] S.T. Ceyer, Annual Review of Physical Chemistry 39 (1988) 479.
[6] C.G. Gu, V.H. Wysocki, Journal of the American Chemical Society 119 (1997) 12010.
[7] J.W. Shen, C. Evans, N. Wade, R.G. Cooks, Journal of the American Chemical Society 121 (1999) 9762.
[8] T. Pradeep, J.W. Shen, C. Evans, R.G. Cooks, Analytical Chemistry 71 (1999) 3311.
[9] M. Deimel, H. Rulle, V. Liebing, A. Benninghoven, Applied Surface Science 134 (1998) 271.
[10] J.C. Vickerman, D. Briggs, Surface Analysis by Mass Spectrometry (2001) 789.
[11] W. Eckstein, H. Verbeek, S. Datz, Applied Physics Letters 27 (1975) 527.
[12] T.M. Bernhardt, B. Kaiser, K. Rademann, Physical Chemistry Chemical Physics 4 (2002) 1192.
[13] J. Zabka, Z. Dolejsek, J. Roithova, V. Grill, T.D. Mark, Z. Herman, International Journal of Mass Spectrometry 213 (2002) 145.
[14] D.C. Jacobs, Journal of Physics—Condensed Matter 7 (1995) 1023.
[15] D.C. Jacobs, Annual Review of Physical Chemistry 53 (2002) 379.
[16] H.D. Hagstrum, Physical Review 96 (1954) 325.
[17] H.D. Hagstrum, Physical Review 96 (1954) 336.
[18] H.D. Hagstrum, Physical Review 122 (1961) 83.
[19] K.J. Snowdon, R. Hentschke, A. Naermann, W. Heiland, Surface Science 173 (1986) 581.
[20] W. Heiland, U. Imke, S. Schubert, K.J. Snowdon, Nuclear Instruments & Methods in Physics Research, Section B: Beam Interactions with Materials and Atoms B27 (1987) 167.
[21] J. Los, J.J.C. Geerlings, Physics Reports 190 (1990) 133.
[22] A. Naermann, W. Heiland, R. Monreal, F. Flores, P.M. Echenique, Physical Review B: Condensed Matter and Materials Physics 44 (1991) 2003.
[23] D.A. Dahl, International Journal of Mass Spectrometry 200 (2000) 3.
[24] W.C. Wiley, I.H. McLaren, Review of Scientific Instruments 26 (1955) 1150.
[25] M. Nolde, K.M. Weitzel, C.M. Western, Physical Chemistry Chemical Physics 7 (2005) 1527.
[26] M. Nolde, Multiphoton-ionization spectroscopy of ammonia and methylamine. Dissertation, Philipps-Universität Marburg, 2006.
[27] Y. Ferro, A. Allouche, F. Cora, C. Pisani, C. Girardet, Surface Science 325 (1995) 139.
[28] H. Waiczies, Construction and test of a new ion-guide-system for ion-molecule-reactions. Dissertation, Freie Universität Berlin, 2003.
[29] D. Van Pijkeren, J. Van Eck, A. Niehaus, Chemical Physics 95 (1985) 449.
[30] W.E. Conaway, T. Ebata, R.N. Zare, Journal of Chemical Physics 87 (1987) 3453.
[31] R. Wörgötter, V. Grill, Z. Herman, H. Schwarz, T.D. Mark, Chemical Physics Letters 270 (1997) 333.
[32] R. Worgotter, J. Kubista, J. Zabka, Z. Dolejsek, T.D. Mark, Z. Herman, International Journal of Mass Spectrometry 174 (1998) 53.